Behavior of electron-irradiation-induced defects in GaAs

D. Stievenard and X. Boddaert
Laboratoire de Physique des Solides, Institut Supérieur d'Electronique du Nord, 41 boulevard Vauban, 59046 Lille CEDEX, France

J. C. Bourgoin and H. J. von Bardeleben
Groupe de Physique des Solides de l'Ecole Normale Supérieure Université de Paris VII, Tour 23, 2 place Jussieu, 75251 Paris CEDEX 05, France

(Received 28 September 1989)

In GaAs, electron irradiation is known to produce vacancy-interstitial pairs in the arsenic sublattice (V_{As}-As_i). The associated levels are electron traps (labeled $E1$–$E5$), and hole traps (labeled $H0$ and $H1$). In addition, complexes (labeled $H2$–$H5$) involving the As_i and residual impurities are created in p-type GaAs. This different behavior between n- and p-type materials is found to be related to a difference in the mobility of As_i during the irradiation. The existence of the various levels observed for the V_{As}-As_i pair corresponds to a distribution in distance between V_{As} and As_i. Most of the pairs are correlated in n-type material while in p-type material a large fraction of the pairs are uncorrelated. In order to verify this picture we have performed a study of the pair distribution versus the flux of irradiation in n- and p-type materials and versus the irradiation dose in p-type material. In p-type material, these studies confirm that the defect labeled $H1$ is a primary defect and the defects $H2$, $H3$, and $H4$ are complexes. The large diffusion length of As_i explains the observed creation rates and the annealing behaviors of these defects. In n-type material, a partial annealing of the defects $E1$–$E5$ is observed under high flux of irradiation because the mobility of As_i is then enhanced by the holes injected during the irradiation. Both this ionization-enhanced annealing and the thermal annealing (which occurs around 200 °C) can be understood in detail. A careful analysis of the kinetics of the pair annihilation and in particular the asymptotic behavior of these kinetics allows the determination of the fraction of correlated pairs and the evaluation to some extent of the distribution in distance of the pairs. Finally these conclusions allow us to propose a microscopic model for the defect $E3$, resulting from the interaction of As_i located at an average distance of 8 Å from the arsenic vacancy.

I. DEFECTS IN ELECTRON-IRRADIATED GaAs

Defects produced by electron irradiation in GaAs have been the subject of a large number of works (see Refs. 1–5 for reviews). In n-type GaAs, it has been demonstrated that the majority-carrier traps, detected by deep-level transient spectroscopy (DLTS) and labeled $E1$–$E5$, are associated with intrinsic primary defect pairs because

(1) The total defect introduction rate, i.e., the sum of the introduction rates of all the traps (~ 4 cm^{-1} at 1 MeV) is equal to the calculated one, assuming the defects belong to only one sublattice.[1]

(2) They are created[1] at the lowest temperature (4 K) with identical introduction rates, however the material has been grown, the nature and the concentration of the residual and doping impurities.

(3) All the traps anneal around 200 °C, with the same first-order kinetics and the annealed fraction is nearly 100%, as expected for close vacancy-interstitial pairs[6] when the defect concentration is small.

(4) The energy liberated[7] during this annealing [8 eV (Ref. 7) per defect] is equal to the theoretical estimation of the energy stored in vacancy-interstitial pairs.[8]

(5) Finally, the study of the orientation dependence of the introduction rate of the defects $E1$, $E2$, and $E3$ has shown a strong anisotropy of their introduction rate due to the interaction of the displaced atom with its nearest neighbors, demonstrating unambiguously by that these E defects belong to the As sublattice.[9] This conclusion has been confirmed by a study of their introduction rate, which is found to be independent of x in $Ga_{1-x}Al_xAs$.[10] The traps observed are thus related to arsenic vacancy-interstitial pairs. In addition, also minority-carrier traps, labeled H0 and $H1$, detected under injection of minority carriers[11] are also created. However, no quantitative study of their introduction rate and their thermal stability has been performed, and it is not possible to know if they are other electronic levels associated with the same defects as the ones giving rise to the E levels.

In p-type GaAs, the $H0$ and $H1$ defects are detected as majority traps, together with other defects $H2$–$H5$, whose presence apparently depend on the nature of the material.[10] It has been shown that $H0$ and $H1$ are also related to the primary defects in the As sublattice,[9] and that the defects $H2$–$H5$ are complexes involving the arsenic interstitial and native impurities.[11] The defects $E1$–$E3$ have also been detected under minority-carriers injection,[11] which implies that V_{As}-As_i pairs are also present and stable in p-type material.

Defects in the Ga sublattice are apparently not detect-

ed by DLTS, and it was first thought[1] that V_{Ga}-Ga_i pairs recombine readily after their creation even at the lowest temperature (4 K). The sublattice to which the defects belong has only been determined for the $E1$, $E2$, $E3$, $H0$, and $H1$ defects: no study of the anisotropy of the introduction rate has been performed for the defects $E4$ and $E5$. These two last defects exhibit DLTS spectra which are superposed and an accurate study of their introduction rate is difficult. However, electron paramagnetic resonance (EPR) measurements have shown[12] that the gallium vacancy is created but is unstable in n-type GaAs, and transforms by the jump of one of its first As neighbors into the As_{Ga}-V_{As} complex. This defect is believed to correspond to the electron trap $E4$.[12]

Thus, when the irradiation dose used is small as is the case in DLTS studies (because the defect concentration must be small compared to the free-carrier concentration), an n-type material contains only primary defects, while a p-type one contains both primary and complex defects. At this stage two questions arise. The first one is: what can explain such difference of behavior? The second question concerns the exact nature of the E defect: why does the V_{As}-As_i pair give rise to such a large series of levels? The aim of this communication is to answer these two questions, providing new data when necessary.

II. THE ARSENIC INTERSTITIAL MOBILITY

A. Migration of As_i under irradiation

In order to explain the different behavior of n- and p-type materials during irradiation, it has been suggested that the mobility of As_i is triggered by the electronic excitation through an athermal mechanism,[13] the existence of which is demonstrated in the case of the E defects by their annealing induced by the injection of minority carriers.[14,15] In such a mechanism the mobility of the interstitial is a function of the rates of electrons and holes trapping on the defect site, i.e., of the level of injection of minority carriers. In case of electron irradiation, the level of injected electron-hole pairs is directly proportional to the flux. In n-type GaAs, for low flux and a low dose of irradiation (usually 10^{15} cm^{-2}) such as the one used for DLTS studies, the As_i mobility is low and thus its diffusion length short. As a result, the created primary defects are closed or correlated V_{As}-As_i pairs, i.e., the distance ρ between the elements of a pair is small compared to the distance R between pairs. For high doses of irradiation (usually 10^{17}–10^{19} cm^{-2}), such as used for EPR or ir absorption studies, the diffusion length of As_i is larger and the creation of complexes through the interaction of mobile As_i with impurities becomes possible. This is indeed observed using EPR, which shows the creation of antisites As_{Ga} through the reaction $As_i + Ga_{Ga} \rightarrow As_{Ga} + Ga_i$,[16–18] or using ir absorption through the creation of B-As_i (Ref. 19) and C-As_i complexes.[20] A larger diffusion length is also observed when the irradiation is performed at high temperature,[21,22] i.e., above 200 °C, the temperature corresponding to the recombination of the pairs (see Sec. IV). In that case, the As_i which escape recombination with their own vacancy can diffuse and create complexes when they get trapped by impurities.

In p-type GaAs, the situation is different: even under low dose (i.e., low flux) of irradiation, the mobility of As_i is already apparently high enough to allow the creation of complexes. In that case, the athermal mobility of As_i is therefore larger. This can be understood if the capture cross section σ_e for electron trapping on the localized level associated with As_i is large compared to the capture cross section σ_h for holes.[23] Indeed, the rate Γ at which carriers are trapped on the defect level is

$$\Gamma = 2[(k_h + g_e)^{-1} + (k_e + g_h)^{-1}]^{-1} , \tag{1}$$

where k_e and k_h are the capture rates, and g_e and g_h are the emission rates for electrons and holes, respectively. At the temperature of irradiation (from room temperature to 4 K), g_e and g_h are small compared with k_e and k_h, so that Γ reduces to

$$\Gamma = 2\frac{k_e k_h}{k_e + k_h} , \tag{2}$$

with

$$k_e = \sigma_e v_e n \tag{3}$$

and

$$k_h = \sigma_h v_h p , \tag{4}$$

where v_e and v_h are the thermal velocities of the electrons and holes. In p-type material the electron concentration n being negligible as compared to the hole concentration p, k_h is far greater than k_e, and Γ can be approximated to

$$\Gamma = 2k_e = 2\sigma_e v_e n , \tag{5}$$

i.e., Γ is directly proportional to σ_e. In n-type material, the same kind of calculation leads to

$$\Gamma = 2k_h . \tag{6}$$

Thus, the mobility induced by the change of the charge state in each material is directly related to the ratio of the electrons and holes capture cross sections.

Another explanation has been recently proposed by Murray *et al.*[24] to explain the formation of the As_i complexes. They suggested that the different behavior of the defects in n- and p-type materials is due to a difference in the stability of the pairs in these two materials. They argue that in n-type GaAs, the pair is stable, whereas in p-type or high-resistivity material, the pair is unstable. Unfortunately, the hypothesis that the pair is not stable in p-type material is in contradiction with the fact that the E defects are also detected in this material[11] as mentioned in Sec. I. Moreover, these authors assume that there is no dependence of the pair stability with the flux of irradiation, in contradiction with the results we shall describe in Sec. III C 2. In Sec. III, we shall provide new direct experimental evidences that the As_i mobility is induced by the irradiation.

B. Thermal stability of the arsenic interstitial

We have some information on the thermodynamic behavior of As_i through the study of the kinetics of the 220 °C stage annealing because it corresponds to As_i mobility. Indeed, it has been shown[25] that the EPR spectrum attributed to the As vacancy, slightly perturbed by the presence of arsenic in neighboring positions, still exists above 250 °C (Fig. 1), whereas it is known that the $E1$–$E3$ and $H0$–$H5$ defects annealed around 220 °C. For low doses of irradiation only Frenkel pairs are created, which completely anneal around 220 °C. On the contrary, for high doses the defects created are pairs, isolated vacancies, and complexes involving As_i and impurities. Thus, only the pairs anneal during a 220 °C annealing, as well as the complexes involving As_i, but the vacancies remain stable. This result is verified by positron-annihilation studies.[26]

Thus, the 220 °C annealing stage is related to the recombination of V_{As}-As_i through the As_i mobility. In such annealing, there are two processes involved in series: first, the migration of the interstitial with a migration energy E_M and second, its jump into the vacancy over a barrier E_R, when it has reached a neighboring interstitial site. Since kinetics are characteristics of the process which limits the reaction when the corresponding rates are sufficiently different, the activation energy associated with the recombination [1.5 eV (Ref. 6)], should therefore be ascribed to E_M or E_R. In p-type GaAs, the annealing behavior of the complexes involving As_i [i.e., the traps $H2$ and $H5$ (Ref. 11)], is characterized by an activation energy of ~ 0.5 eV and a preexponential factor of $\sim 10^3$ s^{-1}, i.e., corresponding to $\sim 10^{10}$ jumps. In that case, the annealing process involves the breaking of the complexes, characterized by an energy E_B, followed by the As_i migration with the energy E_M. As the activation energy does not depend on the complex, it cannot be associated to the breaking energy. Moreover, because 10^{10} jumps are characteristic of a long-range migration, it is the last process which limits the reaction. Thus, the activation energy E_M of the migration of As_i is 0.5 eV (assuming that E_B is small compared with E_M) and, consequently, the barrier E_R for the recombination with the vacancy should be ranging from 1 to 1.5 eV.

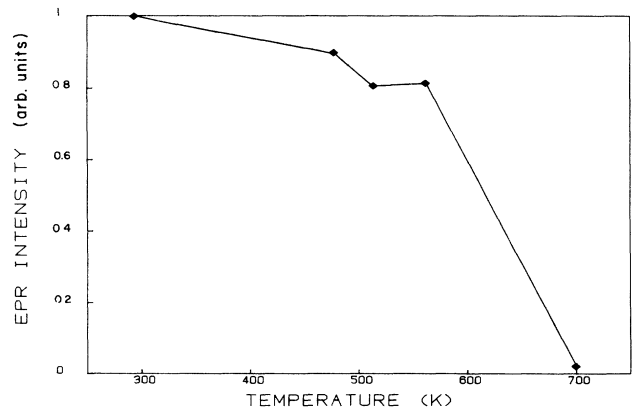

FIG. 1. Relative amplitude of the EPR spectrum associated with V_{As} vs annealing temperature in an n-type doped GaAs material irradiated at room temperature with 10^{17}-cm^{-2} 1-MeV electrons.

III. EVIDENCE FOR THE MOBILITY OF As_i

A. Introduction

We have seen above that the correlation and the annealing kinetics of the defects between n- and p-type materials can be understood in terms of a distribution of pairs, i.e., of pairs whose distance ρ between their two elements V_{As} and As_i is variable depending upon the conditions of irradiation. In n-type material and for a low dose (i.e., small time) of irradiation, because As_i mobility is small, we expect a majority of correlated pairs, i.e., of pairs for which ρ is small compared to the average distance R between two pairs. This is indeed verified, since the thermal annealing kinetics is first order.[6] The fraction of uncorrelated pairs, for which $\rho \lesssim R$, remains small. This fraction can be obtained by looking at the end of the thermal annealing kinetics. This will be done in Sec. IV A 1.

Here, in order to demonstrate clearly the existence of such a distribution of pairs and to verify the existence of the ionization-induced interstitial mobility, we have performed a study of the evolution of the pair distribution versus the conditions of irradiation. For this, we have studied the introduction rates of each trap detected by DLTS, related to pairs of different configurations, versus the flux of irradiation in n- and p-type materials. The ionization (i.e., the number of electrons and holes created) during the irradiation being proportional to the flux, one expects, when the flux increases, and if the hypothesis of the ionization induced mobility is true, to observe a variation in the pair distribution, i.e., in the introduction rates of the different traps relative to each other. This has been complemented by a study of the trap-introduction rates versus dose in p-type material. The diffusion length being proportional to the time t of irradiation, i.e., to the dose at constant flux,[11] the introduction rates of both the primary ($H1$) and the complex defects ($H2$–$H5$) directly related to the distribution of the pairs must change relative to each other when t increases.

We shall see that these studies confirm the existence of a distribution of pairs. The series of E and H defects must be related to pairs in different configurations, from close V_{As}-As_i pairs to uncorrelated ones and isolated V_{As}. Only for the defect $E4$ is this analysis not positive, in agreement with the suggestion that this defect is associated with the antisite defect (As_{Ga}) originating from a transformation of the gallium vacancy.[16]

B. Experiment

For the study of defects in p-type material, the samples used are n^+-p diodes, where the p layer is grown by vapor-phase epitaxy (VPE) and doped with 3.5×10^{16} Zn cm^{-3}. Before irradiation, the samples contain the so-called $HL3$ defect,[27] with a concentration of the order

6×10^{14} cm^{-3}. After irradiation, the contribution of this defect to the DLTS spectrum was systematically subtracted to avoid any error on the measurement of the defect concentrations. This is important in case of the $H3$ defect whose associated DLTS peak is just superimposed on the $HL3$ one.[11] The introduction rates of each individual defect, detected by DLTS have been studied versus the flux of irradiation in the range 0.1–15 μA cm^{-2}, for a constant dose of 10^{15} cm^{-2}. A similar study versus the dose has been also performed. In that case, the flux was fixed to 1 μA cm^{-2}, with doses ranging from 10^{15} to 3×10^{16} cm^{-2}.

For the study of defects in n-type material, the samples were p^+-n diodes where the n-type layer is elaborated by VPE and doped with 10^{16} S cm^{-3}. Before irradiation, no defect is detected in the n-type layer. The irradiations were performed at 1 MeV, with a constant dose of 5×10^{14} cm^{-2}, and fluxes varying in the range 0.1–15 μA cm^{-2}. To avoid any thermal annealing during the irradiation (in case of high fluxes), the samples were mounted on a copper plate cooled with water. The control of the temperature was performed using a thermocouple mounted on the same copper plate and glued in the same way as the sample. For the highest flux used, the time of irradiation was so short that an equilibrium temperature could not be reached: the temperature was about 180 °C at the end of the irradiation, i.e., only for a few seconds. Since the rate of thermal annealing is known,[28] we have deduced that such a thermal effect induces an annealing which corresponds to a 5% decrease in the defect concentration, and is therefore negligible compared to the observed effects.

C. Results

1. Flux and dose dependences in p-type material

All the defects detected are the well-known H defects: this has been verified by studying the variations of their emission rates versus temperature (the so-called signature of the defects). The associated activation energies indicate that the defect levels are located at $E_V+0.25$ eV, $E_V+0.42$ eV, $E_V+0.54$ eV, $E_V+0.79$ eV, and $E_V+0.85$ eV above the valence band E_V for the $H1$–$H5$ defects, respectively.[11] No dependence on the flux has been detected, which is consistent with the fact that, the As_i mobility being large, the steady state is reached even for low fluxes.

Figure 2 shows the concentration of the defects $H1$–$H4$ versus dose: the concentration of $H1$ grows linearly with the dose, as expected in the case of a primary defect;[29] its creation rate is ~0.1 cm^{-1}. As to the defects $H2$–$H4$, their concentrations versus dose can be understood by the fact that As_i are mobile during the irradiation and get trapped on impurities, thus confirming that they are complexes. Indeed, the number of created complexes must be proportional to Dt,[30] where D is the diffusion coefficient of As_i, constant since the flux was kept low and constant (1 μA cm^{-2}). The concentration of a complex saturates when the corresponding impurities are exhausted. The defect $H2$ grows linearly and

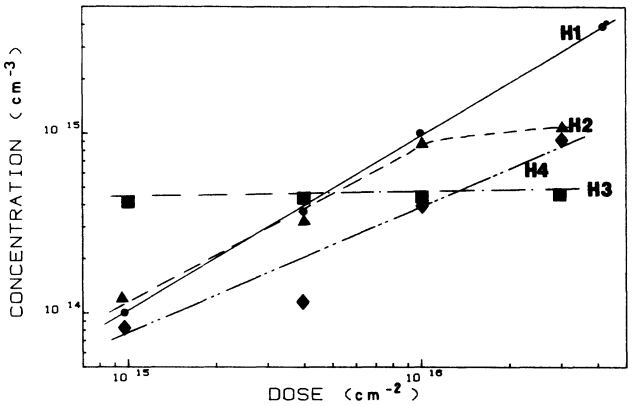

FIG. 2. Concentration of the $H1$–$H4$ defects vs the dose of irradiation.

then saturates: the concentration at saturation, $\sim10^{15}$ cm^{-3}, is of the order of the Cu concentration, in agreement with the suggestion that Cu is involved in the creation of this defect.[31,32] The defect $H3$ remains constant, implying that the first dose used is large enough to saturate the impurity involved [which could be Fe (Ref. 10)]. Only the defect $H4$ seems to grow linearly in the whole dose range. However, this defect must not be analyzed as a primary defect as $H1$. Indeed, a previous study of its thermal annealing[11] shows it is also a complex defect, since it exhibits the same annealing kinetics as $H2$ and $H3$. Simply, it does not saturate because the impurity involved in its formation is larger than 10^{15} cm^{-3}.

In conclusion, the behavior of the defect-introduction rates confirms the primary nature of the defect $H1$, and the complex nature of the defects $H2$–$H4$, due to the high mobility of As_i in p-type material.

2. Flux dependence in n-type material

Figure 3 shows two typical spectra obtained for the same irradiation dose and two fluxes, 0.1 and 10 μA cm^{-2}. Because the concentration of the defects is

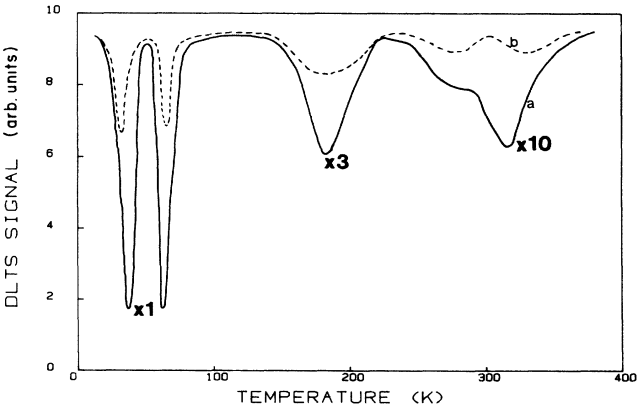

FIG. 3. DLTS spectra of the E defects in n-type GaAs vs the flux of irradiation: a, $\Phi=0.1$ μA cm^{-2}; b, $\Phi=10$ μA cm^{-2} for the same dose of irradiation (10^{15} cm^{-2}, 1 MeV).

smaller in the sample irradiated with a large flux than in the sample irradiated with the low flux, this indicates that a partial recombination of the V_{As}-As_i pairs has taken place. Their introduction rates are of the order of the usual ones,[1] as long as the flux is less than 10 $\mu A\,cm^{-2}$. For this flux, the rates decrease. We can see that the rates of the $E1$ and $E2$ defects decrease in the same fashion, which confirms they are two levels of the same defect.[1] Moreover, as can be seen in Fig. 3, the relative concentrations of all the defects vary with the flux. As discussed previously, this can be interpreted in the following way: under high flux, the ionization becomes non-negligible, thus allowing an increase in the As_i mobility, with the result that the pair distribution changes its shape.

IV. THE PAIR DISTRIBUTION

A. Thermal annealing

We consider now the thermal annealing of the defects. It has been performed by Pons *et al.*[28] in *n*-type GaAs, and Stievenard *et al.*[11] in *p*-type GaAs. The kinetics have been analyzed: they are first order, as expected for a recombination of correlated pairs. However, if there is a distribution in distance ρ between the elements of the pairs, then one expects only the short distance (correlated) pairs to anneal with first-order kinetics. As to the uncorrelated pairs, they should recombine through a diffusion-limited process. For uncorrelated pairs, it can be shown[29,32] that the annealed fraction behaves, with the annealing time t, as $t^{-1/2}$. We therefore analyzed the end of the annealing kinetics of the E traps which are related to primary defects, i.e., $E2$, $E3$, $E5$, and $H1$ (the annealing of $E1$ is identical to that of $E2$, since these two traps are related to the same defect). The annealed fraction which varies linearly with $t^{-1/2}$ will provide the fraction of the uncorrelated pairs. As to the annealing kinetics of the $H2$, $H3$, and $H4$ traps which are related to complexes involving As_i, they should provide the migration energy of As_i.

1. The E defects

Let us first recall some details concerning the thermal behavior of the E defects. A fraction of the $E2$ defect labeled $E2''$, exhibits a slow annealing, while the remaining fraction labeled $E2'$ has a faster annealing rate identical to the one of $E3$ and $E5$. However, both slow and fast annealings are characterized by the same activation energy (1.55 ± 0.15 eV). We have analyzed the end of the annealed fraction for each defect. As illustrated in Fig. 4, this fraction varies indeed as $t^{-1/2}$ for $E2''$. The analysis of the diffusion process versus temperature, in terms of a diffusion coefficient D, is given in Fig. 5 for $E2''$. The slope of this curve gives the activation energy E_a associated with the annealing process. As to the extrapolation of this curve to $T^{-1}=0$, it gives the preexponential factor ν_0, which determines the number of jumps N_j the interstitial should make in order to recombine with its vacancy. For the $E2''$ defect, $E_a=0.40\pm0.08$ eV, and ν_0 is the order of 0.1 s^{-1}, which implies $N_j\sim10^{13}$. The same

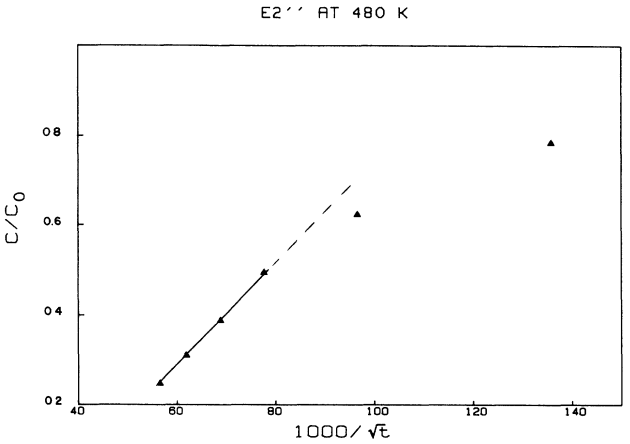

FIG. 4. Annealing behavior of the $E2''$ trap vs $t^{-1/2}$ at 480 K.

analysis cannot be performed for the $E2'$, $E3$, and $E5$ defects: the end of the annealing fraction does not behave as $t^{-1/2}$.

These results can be understood in the following way. The traps $E2'$, $E3$, and $E5$ correspond to closed pairs, and the process involved in their annealing is associated with a jump over a barrier (1.55 eV) for the recombination and not with a diffusion mechanism. This is in agreement with the fact that the annealing kinetics is first order even for long times. On the contrary, the trap $E2''$ corresponds to uncorrelated pairs for which the annealing is limited by diffusion: the number of jumps is high. Consequently, the associated activation energy (~0.40 eV) must be ascribed to As_i mobility. Finally, as shown in Fig. 4, the fraction of correlated pairs is $\sim50\%$.

2. The H defects

The annealing kinetics of the $H1$–$H4$ defects have been described in Ref. 11. For all traps, the kinetics contains two regimes: a fast one followed by a slow one, in a similar fashion as for the $E2$ defect. The origin of these two regimes has been ascribed to a variation of the associated activation energy with the charge state of the

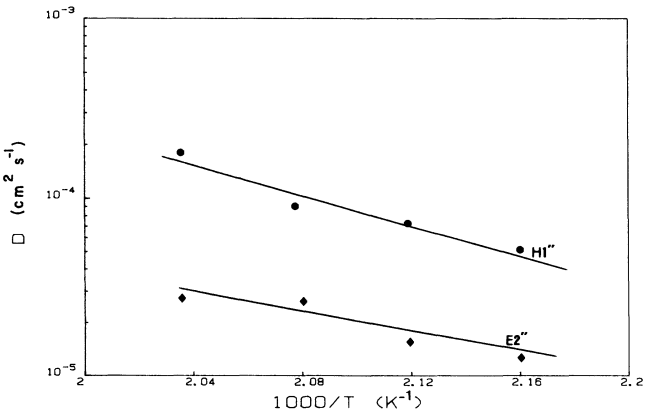

FIG. 5. Diffusion coefficient D associated with the annealing of the $E2''$ and $H1''$ traps vs the inverse of the temperature.

mobile defect, the Fermi level moving as the annealing proceeds. We consider first the $H1$ trap which is known to correspond to the V_{As}-As_i pair. As shown in Fig. 6, the end of the slow part, labeled $H1''$, behaves as $t^{-1/2}$. The kinetics can then be analyzed in terms of a diffusion process, as illustrated in Fig. 5, and the activation energy E_a associated with the process is $E_a=0.51\pm0.08$ eV, with a preexponential factor ν_0 of the order of 10^3, i.e., a number N_j of jumps of the order of 10^{10}. This behavior is therefore very similar to the one of the $E2''$ trap. It thus gives for the activation energy associated with the mobility of As_i in p-type material a value slightly different than in n-type material. This is not surprising, because such activation energy is expected to depend on the defect charge state. Figure 6 indicates that the fraction of uncorrelated pairs is $\sim 40\%$. As to the fast annealing of the trap $H1$, labeled $H1'$, it has the same behavior as the $E2',E3,E5$ group, i.e., is first order and does not exhibit a linear variation with $t^{-1/2}$ at long times. Finally, the analysis of the kinetics of the complexes traps $H2$–$H4$, is unfortunately not clear, and does not allow a rigorous conclusion. The behavior versus $t^{-1/2}$ is quasilinear, and gives a number of jumps of $\sim 10^{7\pm2}$, in accordance with a long-range diffusion. No quantitative conclusion can be obtained for the associated activation energies. Presumably, the situation is more complicated because there are several superimposed mechanisms: dissociation of complexes, migration of As_i, and Fermi-level effect on the mobility.

3. Conclusion

The analysis of the annealing kinetics shows that irradiation with low doses produces a majority of closed pairs in n-type material, which are the traps $H3$ and $H5$ and the fraction $E2'$ of the $E2$ traps. Only a fraction ($\sim 50\%$) of this last trap are uncorrelated pairs. This result implies that the pair distribution is rather narrow, i.e., that the As_i mobility is small, a conclusion which reinforces the picture we have deduced previously. In p-type material, only a small fraction of the defects produced are closed pairs.

B. Irradiation-induced annealing

We now examine the effect of the irradiation flux on the pair distribution in order to determine the induced variation on the mobility of As_i. Under high flux, it is expected that, according to an athermal mechanism,[13–15] the ionization increases the mobility of the interstitial, and, consequently, that the distribution of the pairs will be modified. For this, we consider only the two main defects $E2$ and $E3$, since $E1$ corresponds to the same defect as $E2$, and $E4$ is not attributed to a simple pair. As for $E5$, it is in low concentration and can be neglected in a simplified model.

For an irradiation with a low flux, the concentrations of the $E2$ and $E3$ defects are directly proportional to the dose, with introduction rates ν_2 and ν_3, respectively. Under a high flux Φ the As_i mobility is enhanced and a fraction of the pairs recombine, with rates r_2 and r_3, respectively. Then the behavior of the defect concentrations $[E2]$ and $[E3]$ is represented by the following equations:

$$\frac{d[E2]}{dt}=\nu_2\Phi-r_2[E2]\ , \tag{7}$$

$$\frac{d[E3]}{dt}=\nu_3\Phi-r_3[E3]\ , \tag{8}$$

with the initial conditions $[E2]=[E3]=0$ at $t=0$. The solutions of Eqs. (7) and (8) are

$$[E2]=\frac{\nu_2\Phi}{r_2}[1-\exp(-r_2t)] \tag{9}$$

and

$$[E3]=\frac{\nu_3\Phi}{r_3}[1-\exp(-r_3t)]\ . \tag{10}$$

The introduction rates ν_2 and ν_3 being known[1] from the concentrations measured by the DLTS technique and the time t being fixed experimentally, it is easy to deduce the variation of the annealing rates r_2 and r_3 for each value of Φ by a fit of the experimental data with the relations (9) and (10). The results of these fits are given in Figs. 7 and 8 and the variations of r_2 and r_3 versus Φ are given

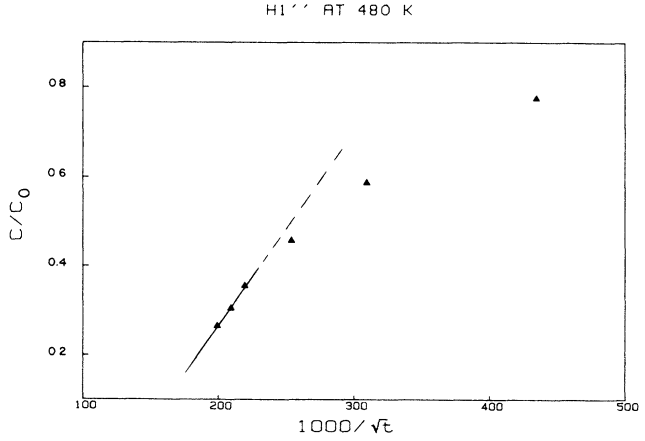

FIG. 6. Annealing behavior of the $H1''$ trap vs $t^{-1/2}$ at 480 K.

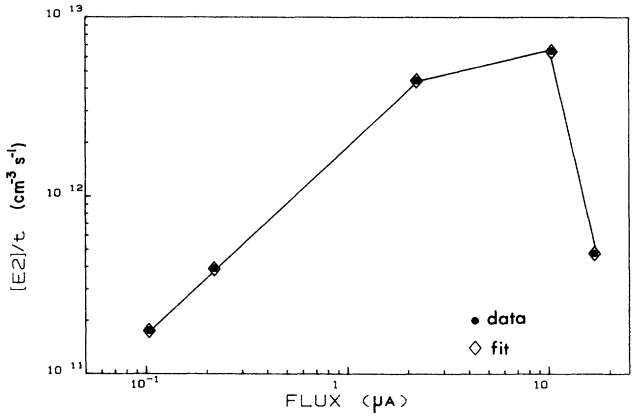

FIG. 7. $[E2]/t$ vs the flux of irradiation.

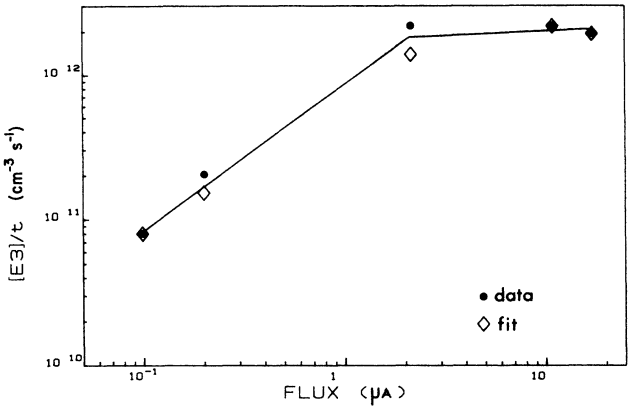

FIG. 8. $[E3]/t$ vs the flux of irradiation.

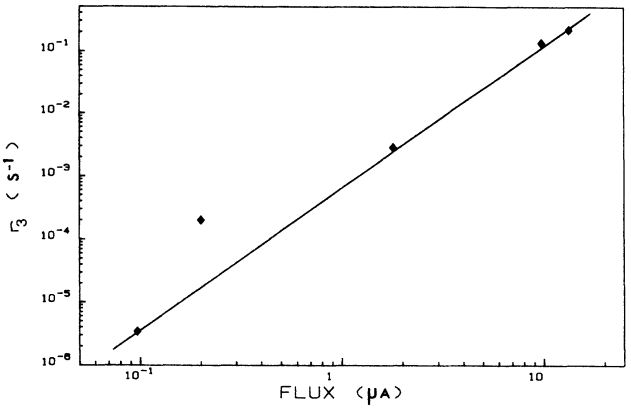

FIG. 10. Annealing rate r_3 of the $E3$ defect vs the flux of irradiation.

in Figs. 9 and 10. These last figures demonstrate clearly that the annealing rates increase with the flux in accordance with an ionization-induced mobility of the As_i.

V. A MICROSCOPIC MODEL FOR THE VARIOUS TRAPS

It is now interesting to see if the pair distribution obtained qualitatively by the preceding analysis is coherent with the characteristics of the defects, i.e., if the energy levels associated with all the observed traps vary accordingly with the distribution in distance of the vacancy-interstitial pair.

Since we know that the $E1$ and $E2$ traps are two levels of the same defect and attributed to the isolated As vacancy using theoretical considerations,[33] we consider that $(E1,E2)$ are two levels of the isolated V_{As}, i.e., with As_i at a distance such that it does not perturb significantly its energy level. Then the $E3$ and $E5$ defects correspond to different states of V_{As} which are perturbed as As_i located at smaller distances. This picture is consistent with the energy distribution of the levels. Indeed, the interaction

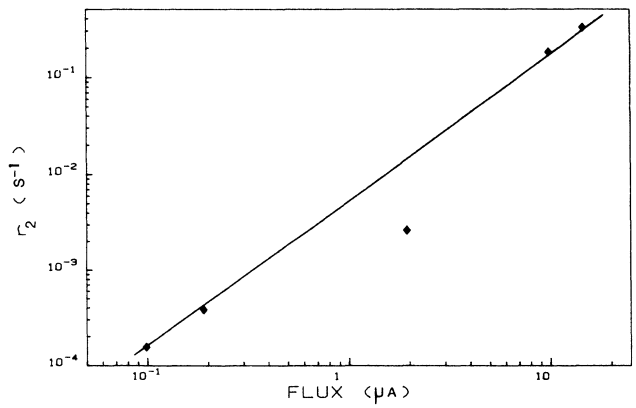

FIG. 9. Annealing rate r_2 of the $E2$ defect vs the flux of irradiation.

ΔE of the As_i must result in a shift of the energy level with respect to the $E2$ level, making the trap level deeper.

We do not know the exact nature of the interaction. However, for large enough distances, it should take the form of a screened Coulomb interaction $e^2/\epsilon\rho$, where ϵ is the dielectric constant of the material. In Table I we calculate the shift in the ionization energies $\Delta E_j = E_j - E2$ of the E defects, deduced from their signatures, corrected eventually by the activation energy E_B associated with the capture cross section.[1] Using these values we can deduce ΔE_j, and then the corresponding distance ρ_j assuming a Coulomb interaction. As shown in the table, we obtain for the trap $E3$ a distance of ~ 7 Å, in which case the interaction can indeed reasonably be described by a Coulomb field. However, in case of $E5$ the Coulomb interaction cannot be the correct interaction potential to account for the value of ΔE_j, the distance ρ deduced being too short.

In order to verify if the distance found for $E3$ is reasonable, we have made a correlation between the associated DLTS spectrum and the simulated DLTS spectrum corresponding to the family of defects, i.e., of pairs, for all the possible sites of As_i around V_{As}. For each As_i site we determine ΔE_j, assuming a Coulomb interaction. In the simulation, two parameters are used: N_T, the consideration of the distribution of all the equivalent sites situated at a given distance ρ and σ, the capture cross sec-

TABLE I. Energy levels and distances ρ_j $(j=2,3,5)$ between V_{As} and As_i for the Ej defects, deduced using a model of Coulomb interaction.

	$E2$	$E3$	$E5$
E_A (eV)	0.14	0.4	0.96
E_B (eV)	0	0.1	~0.3
E_j (eV)	0.14	0.3	~0.66
ΔE_j (eV)	0	0.16	~0.52
ρ_j (Å)	∞	6.9	2.1

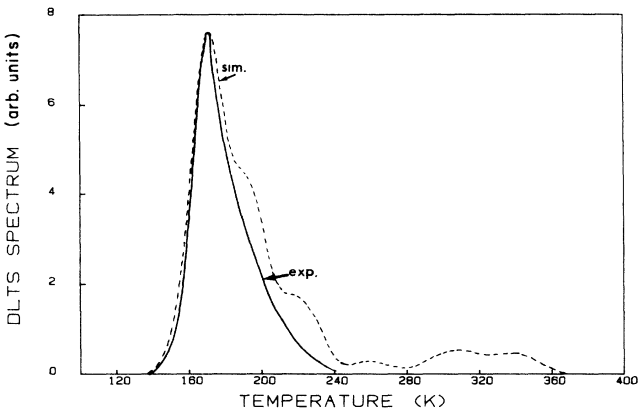

FIG. 11. Comparison between the simulated (sim.) DLTS spectrum of the $E3$ defect and the experimental (exp.) one.

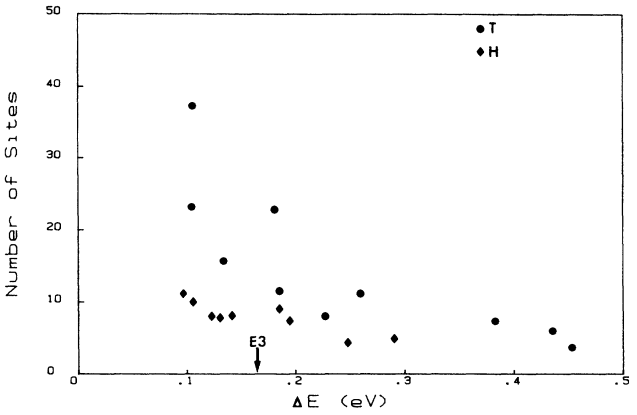

FIG. 12. Distribution of the interstitial sites (T, tetrahedral; H, hexagonal) vs the Coulomb interaction ΔE_j.

tion, assumed to be constant (equal to 10^{-15} cm^2, a typical value for the E defect). The value of σ is not of prime importance for the simulation: it just shifts in temperature all the various DLTS peaks by the same quantity. We have made the simulation using the 204 tetrahedral and hexagonal interstitial sites nearest to the vacancy (i.e., ΔE_j, ranging from 0.1 to 0.5 eV). The comparison between the experimental and the simulated DLTS spectrum is given in Fig. 11. It appears clearly that a fit is obtained only for the simulated peak corresponding to interstitials on tetrahedral sites located at ρ ranging around 7–8 Å (see Fig. 12).

Consequently, this simulation allows us to propose that the trap $E3$ is related to a distribution of interstitials on tetrahedral sites, and located at an average distance of $\sim$8 Å from the vacancy.

VI. CONCLUSION

This work allows a comprehensive understanding of the defects introduced by electron irradiation in GaAs. Using complementary studies of the introduction of the various defects versus dose, flux, and thermal annealing in n- and p-type materials, we demonstrated that the behavior of these defects is essentially bound to the mobility of As_i. In n-type GaAs, we found that the mobility of As_i increases with the flux, and that it is high enough to induce the creation of both primary defects and complexes involving As_i and some impurity in p-type materials. The primary defects observed are associated with a distribution of correlated and uncorrelated pairs, i.e., with variable distances between V_{As} and As_i, which explains the series of associated levels.

[1]D. Pons and J. C. Bourgoin, J. Phys. C **18**, 3839 (1985).
[2]D. V. Lang and L. C. Kimerling, in *International Conference on Lattice Defects in Semiconductors, Freiberg, Germany, 1974,* IOP Conf. Proc. No. 23 (IOP, London, 1975), Vol. 23, p. 581.
[3]D. V. Lang, in *International Conference on Prediction Effects in Semiconductors, Dubrovnik, 1976,* IOP Conf. Proc. No. 31, edited by N. B. Urli and J. W. Corbett (IOP, Bristol, 1977), p. 70.
[4]A. Mircea and D. Bois, in *International Conference on Radiation Effects in Semiconductors, Nice, 1978,* IOP Conf. Proc. No. 46, edited by J. H. Albany (IOP, London, 1979), p. 82.
[5]J. C. Bourgoin, H. J. von Bardeleben, and D. Stievenard, Phys. Status Solidi A **102**, 499 (1987).
[6]D. Pons, A. Mircea, and J. C. Bourgoin, J. Appl. Phys. **51**, 4150 (1980).
[7]H. Lim, H. J. von Bardeleben, and J. C. Bourgoin, Phys. Rev. Lett. **58**, 2315 (1987).
[8]G. A. Baraff and M. Schlüter, Phys. Rev. Lett. **55**, 1327 (1985).
[9]D. Pons and J. C. Bourgoin, Phys. Rev. Lett. **47**, 1293 (1981).
[10]S. Loualiche, A. Nouailhat, G. Guillot, M. Gavand, A. Laugier, and J. C. Bourgoin, J. Appl. Phys. **53**, 8691 (1982).
[11]D. Stievenard, X. Boddaert, and J. C. Bourgoin, Phys. Rev. B **34**, 4048 (1986).
[12]H. J. von Bardeleben, J. C. Bourgoin, and A. Miret, Phys. Rev. B **34**, 1360 (1986).
[13]J. C. Bourgoin and J. W. Corbett, Radiat. Effects **36**, 157 (1978).
[14]D. Stievenard and J. C. Bourgoin, Phys. Rev. B **33**, 8410 (1986).
[15]D. V. Lang and C. H. Henry, Phys. Rev. Lett. **35**, 1525 (1975).
[16]H. J. von Bardeleben and J. C. Bourgoin, J. Appl. Phys. **58**, 1041 (1985).
[17]R. B. Beall, R. C. Newman, J. E. Whitehouse, and J. Woodhead, J. Phys. C **18**, 3273 (1985).
[18]N. K. Goswani, R. C. Newman, and J. E. Whitehouse, Solid State Commun. **40**, 473 (1981).
[19]M. R. Brozel and R. C. Newman, J. Phys. C **8**, 243 (1978).
[20]F. Thomson, S. R. Morrison, and R. C. Newman, in *International Conference on Radiation Damage and Defects in Semiconductors, Reading, England, 1972,* IOP Conf. Proc. No. 16, (IOP, London, 1973), p. 371.
[21]D. Stievenard, J. C. Bourgoin, and D. Pons, Physica B + C

116B, 394 (1983).
[22]D. Stievenard and J. C. Bourgoin, J. Appl. Phys. **59**, 743 (1986).
[23]J. C. Bourgoin and M. Lannoo, *Point Defects in Semiconductors II, Experimental Aspects* (Springer, Berlin, 1983), Chap. 7.
[24]R. Murray, R. C. Newman, and J. Woodhead, Semicond. Sci. Technol. **2**, 399 (1987).
[25]H. J. von Bardeleben and J. C. Bourgoin, Phys. Rev. B **33**, 2890 (1986).
[26]J. C. Bourgoin, H. J. von Bardeleben, and D. Stievenard (unpublished).
[27]A. Mitonneau, G. M. Martin, and A. Mircea, Electron. Lett. **13**, 666 (1977).
[28]D. Pons, P. M. Mooney, and J. C. Bourgoin, J. Appl. Phys. **51**, 2038 (1980).
[29]Reference 23, Chap. 9.
[30]D. V. Lang and R. A. Logan, J. Electron. Mater. **4**, 1053 (1975).
[31]H. P. Gislason, P. G. Wang, and B. Monemar, J. Appl. Phys. **58**, 240 (1985).
[32]J. C. Bourgoin, and F. Mollot, Phys. Status Solidi B **43**, 343 (1971).
[33]S. Loualiche, A. Nouaillhat, G. Guillot, and M. Lannoo, Phys. Rev. B **30**, 5822 (1984).